


Finite-size corrections of defect energy levels involving ionic polarization

 Stefano Falletta¹, Julia Wiktor,² and Alfredo Pasquarello¹
¹Chaire de Simulation à l'Echelle Atomique (CSEA), Ecole Polytechnique Fédérale de Lausanne (EPFL), CH-1015 Lausanne, Switzerland

²Department of Physics, Chalmers University of Technology, SE-412 96 Gothenburg, Sweden

 (Received 27 November 2019; revised 20 February 2020; accepted 26 June 2020; published 17 July 2020)

We develop a scheme for finite-size corrections of vertical transition energies and single-particle energy levels involving defect states with built-in ionic polarization in supercell calculations. The method accounts on an equal footing for the screening of the electrons and of the ionic polarization charge arising from the lattice distortions. We demonstrate the accuracy of our corrections for various defects in MgO and in water by comparing with the dilute limit achieved through the scaling of the system size. The general validity of our formulation is also confirmed through a sum rule that connects vertical transition energies with the formation energies of structurally relaxed defects.

DOI: 10.1103/PhysRevB.102.041115

Interest in optical transitions involving defect states has been growing in recent years for their potential in optoelectronic and photovoltaic applications [1–4]. In this context, density functional theory calculations subject to periodic boundary conditions represent the method of choice for studying defect properties [5]. However, in a supercell, the long-range nature of the electric field associated with a localized charge leads to spurious finite-size effects on defect formation energies [6,7]. This limitation can be overcome by addressing various supercells of increasing size and extrapolating to the limit of an infinitely large supercell [7–11]. Since this method becomes prohibitive for large systems, it is preferable to apply *a posteriori* model correction schemes [6,7,10,12–14]. Such corrections depend quadratically on the extra electronic charge and scale inversely with the dielectric constant of the material. In this regard, the scheme proposed by Freysoldt, Neugebauer, and Van de Walle (FNV) [6] is highly accurate [7], as illustrated in Fig. 1(a) for the hole polaron in MgO.

However, available model corrections [6,12–14] cannot trivially be applied to vertical transitions, which involve defect charge states in the presence of a frozen lattice distortion. For illustration, we consider in Fig. 1(b) the formation energy corresponding to the neutral state obtained upon vertical electron injection in the hole polaron state of MgO. While current schemes do not give any correction for neutral defects [6,12–14], we observe noticeable scaling. Similarly, in Fig. 1(c), we show that the vertical extraction energy of the hydrated electron scales significantly with the system size, an effect that should be assigned to the neutral state as the negatively charged state is heavily screened ($\epsilon_0 = 78.3$ at ambient conditions [15]). In the absence of a hydrated electron, the water dipoles remain oriented in a frozen geometry, leading to a divergence of the ionic polarization [cf. Fig. 1(d)], which needs to be properly accounted for in correction schemes.

Since vertical transitions only involve electronic relaxations, the spurious interactions in the supercell are expected to be dominated by the high-frequency dielectric constant ϵ_∞ . This generally leads to significantly larger corrections than for relaxed defects. For instance, in a recent study of transition

energies in Ga₂O₃, the choice of the dielectric constant leads to differences up to 1 eV and the issue could not be solved by system size scaling because of the prohibitive computational cost [3].

After the submission of the present work, Gake *et al.* elaborated a formulation for correcting vertical transition

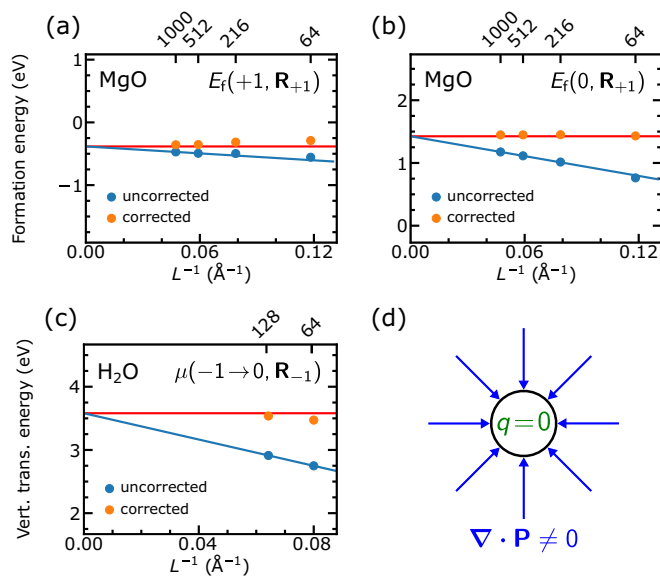


FIG. 1. Scalings with inverse supercell size L^{-1} for (a) the formation energy of the hole polaron in MgO (for $\epsilon_F = 0$), (b) the formation energy of the neutral defect in the geometry of the hole polaron in MgO, and (c) the vertical transition energy for the hydrated electron in water (uncorrected values from Ref. [4]). The number of atoms or water molecules in the supercell is given at the top. The formation energies in the dilute limit are found by linear extrapolation of the two largest supercells and are indicated by horizontal red lines. (d) Schematics pointing to the presence of a divergence in the ionic polarization, $\nabla \cdot \mathbf{P} \neq 0$, due to lattice distortions, which cause finite-size effects even in the absence of an external charge ($q = 0$).

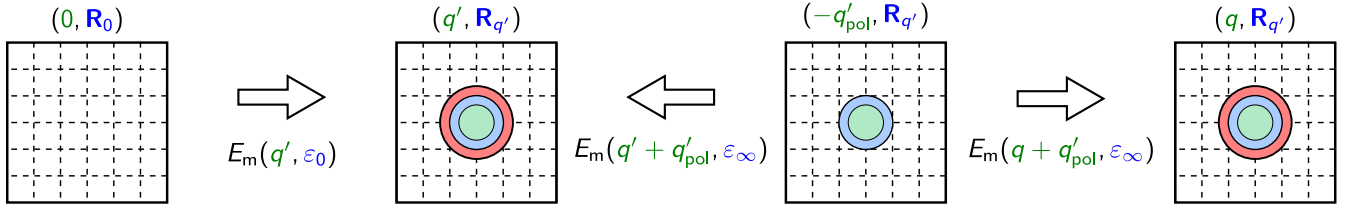


FIG. 2. Schematics for deriving the formula in Eq. (4). The external charge is shown in green, the ionic polarization charge in blue, and the electronic polarization charge in red. The system $(0, \mathbf{R}_0)$ does not show any localized polarization charge and can be used as the starting point for the application of model corrections involving ϵ_0 . Similarly, $(-q'_{\text{pol}}, \mathbf{R}_{q'})$ does not have any electronic polarization charge and can be used as the starting point for model corrections involving ϵ_∞ .

energies [16], which appears to give reasonable numerical results. However, the relation with limiting cases pertaining to existing formulations for structurally relaxed defects has not been established and the correction of single-particle energies appears unsatisfactory [16]. Hence, the validity of this scheme beyond the investigated cases remains to be ascertained.

In this Rapid Communication, we present a method providing finite-size corrections of vertical transition energies and single-particle defect levels in the presence of ionic polarization charges induced by lattice distortions. To address this issue, we focus on the formation energies of defect states electronically relaxed in the presence of a built-in ionic polarization. We show that our scheme gives accurate corrections through extrapolation to the limit of an infinitely large supercell for various defects in MgO and water. As a further validation, we demonstrate that our corrections for vertical transition energies satisfy a sum rule connecting them to state-of-the-art corrections for structurally relaxed defects.

We generalize the notion of formation energy [5,7] to account for a defect in the charge state q within a frozen geometry $\mathbf{R}_{q'}$ as induced by a charge q' ,

$$E_i(q, \mathbf{R}_{q'}) = E(q, \mathbf{R}_{q'}) - E(0, \mathbf{R}_0) + q(\epsilon_F + \epsilon_v) - \sum_i n_i \mu_i + E_{\text{cor}}(q, \mathbf{R}_{q'}), \quad (1)$$

where $E(q, \mathbf{R}_{q'})$ and $E(0, \mathbf{R}_0)$ are total energies, ϵ_v is the valence band maximum, ϵ_F the Fermi level, n_i the number of atoms of species i involved in the defect, and μ_i the respective chemical potential. $E_{\text{cor}}(q, \mathbf{R}_{q'})$ corrects the finite-size effects and constitutes a crucial auxiliary quantity in our formulation.

The correction $E_{\text{cor}}(q, \mathbf{R}_q)$ for a defect in charge state q within a geometry relaxed in the presence of the same charge q can be expressed as

$$E_{\text{cor}}(q, \mathbf{R}_q) = E_m(q, \epsilon_0), \quad (2)$$

where $E_m(q, \epsilon_0)$ corresponds to a regular model correction [6,12–14] for an external charge q screened by the dielectric constant ϵ_0 . Similarly, we define $E_m(q, \epsilon_\infty)$ as the model correction due to the sole electronic screening of the charge q through the high-frequency dielectric constant ϵ_∞ . For instance, the latter correction applies to the case of a charge q in a neutral pristine lattice in which only electronic relaxation is allowed.

Here, we describe the effect of lattice distortions in the configuration $\mathbf{R}_{q'}$ by considering the ionic polarization charge q'_{pol} . This charge can be defined by setting the long-range

screened potential $q'/(\epsilon_0 r)$ equal to $(q' + q'_{\text{pol}})/(\epsilon_\infty r)$. This leads to

$$q'_{\text{pol}} = -q' \left(1 - \frac{\epsilon_\infty}{\epsilon_0} \right). \quad (3)$$

When an external free charge amounting to $-q'_{\text{pol}}$ is inserted at the defect site in the configuration $\mathbf{R}_{q'}$, the electronic polarization vanishes. Hence, the system $(-q'_{\text{pol}}, \mathbf{R}_{q'})$ defined in this way can be used as a starting point for model finite-size corrections involving electronic screening, i.e., governed by ϵ_∞ .

To find an expression for $E_{\text{cor}}(q, \mathbf{R}_{q'})$, we construct the final state through a three-step procedure, as illustrated in Fig. 2. The first step $(0, \mathbf{R}_0) \rightarrow (q', \mathbf{R}_{q'})$ corresponds to the formation of a regularly relaxed defect of charge state q' and is hence described by a correction $E_m(q', \epsilon_0)$ [cf. Eq. (2)]. The second step $(q', \mathbf{R}_{q'}) \rightarrow (-q'_{\text{pol}}, \mathbf{R}_{q'})$ needs a correction corresponding to $-E_m(q' + q'_{\text{pol}}, \epsilon_\infty)$, where the minus sign results from the application of the model correction to the inverted step from $(-q'_{\text{pol}}, \mathbf{R}_{q'})$ to $(q', \mathbf{R}_{q'})$ and $q' + q'_{\text{pol}}$ represents the net localized charge to which the electrons respond. The use of ϵ_∞ is warranted by the purely electronic nature of the screening as the lattice structure $\mathbf{R}_{q'}$ is kept fixed. The last step $(-q'_{\text{pol}}, \mathbf{R}_{q'}) \rightarrow (q, \mathbf{R}_q)$ leads to the final configuration (q, \mathbf{R}_q) and needs a correction $E_m(q + q'_{\text{pol}}, \epsilon_\infty)$, which can be justified analogously to the previous step.

Summing up the corrections pertaining to the three steps, we obtain the correction for a defect of charge q in the frozen equilibrium geometry pertaining to the charge state q' ,

$$E_{\text{cor}}(q, \mathbf{R}_{q'}) = E_m(q', \epsilon_0) - E_m(q' + q'_{\text{pol}}, \epsilon_\infty) + E_m(q + q'_{\text{pol}}, \epsilon_\infty). \quad (4)$$

Equation (4) has a well-defined physical meaning. Indeed, the difference between the first two terms accounts for the finite-size effects due to the establishment of the ionic polarization charge q'_{pol} , while the last term results from the electronic response to the localized charge $q + q'_{\text{pol}}$. Furthermore, our formula in Eq. (4) properly recovers the model corrections for regularly screened defects. When a charge q is in its relaxed structure \mathbf{R}_q , i.e., $q' = q$, the last two terms on the right-hand side of Eq. (4) cancel and the correction reduces to $E_m(q, \epsilon_0)$, as in Eq. (2). Similarly, when the charge q is added to a pristine lattice \mathbf{R}_0 without allowing for ionic relaxation, i.e., taking $q' = 0$ and hence $q'_{\text{pol}} = 0$, the first two terms on the right-hand side of Eq. (4) vanish and $E_m(q, \epsilon_\infty)$ is correctly retrieved.

We now consider the vertical transition energy between the charge states q' and q in the geometry $\mathbf{R}_{q'}$,

$$\mu(q' \rightarrow q, \mathbf{R}_{q'}) = E_f(q, \mathbf{R}_{q'}) - E_f(q', \mathbf{R}_{q'}). \quad (5)$$

Using Eq. (4), we obtain the finite-size correction for this vertical transition,

$$\mu_{\text{cor}}(q' \rightarrow q, \mathbf{R}_{q'}) = E_m(q + q'_{\text{pol}}, \varepsilon_\infty) - E_m(q' + q'_{\text{pol}}, \varepsilon_\infty), \quad (6)$$

where the terms due to the establishment of the ionic polarization charge q'_{pol} cancel and only the terms related with the electronic response to the net localized charge remain. When the charge q' in the initial configuration is neutral, our correction for the vertical transition in Eq. (6) becomes $E_m(q, \varepsilon_\infty)$, which results from purely electronic screening. However, for the general case $q' \neq 0$, the expression in Eq. (6) shows that a complex interplay of ionic and electronic screening occurs. We analytically proved that the formulation for μ_{cor} derived in Ref. [16] coincides with our result in Eq. (6) [cf. Supplemental Material (SM) [17]].

We first demonstrate the accuracy of our scheme for the hole polaron and the oxygen vacancy in MgO. The calculations are performed at the hybrid-functional level [18], as implemented in the CP2K code [19–23]. Computational details and other checks of consistency [24–26] can be found in the SM [17]. By applying a finite electric field [27] to the largest supercell under consideration (1000 atoms), we determine $\varepsilon_0 = 8.6$ and $\varepsilon_\infty = 2.5$, in agreement with the experimental values $\varepsilon_0^{\text{expt}} = 9.8$ [28] and $\varepsilon_\infty^{\text{expt}} = 3.0$ [29]. As the model correction E_m for regularly screened defects, we adopt the FNV method [6]. In Fig. 1(b), we illustrate the quality of our correction scheme for the formation energy $E_f(0, \mathbf{R}_{+1})$ of the neutral charge state in the geometry of the hole polaron. In the case of the oxygen vacancy, we consider $E_f(q, \mathbf{R}_{q'})$ for $q, q' = 0, +1, +2$, resulting in eight cases excluding $E_f(0, \mathbf{R}_0)$, which we take as the reference. Figure 3 shows the scaling towards the dilute limit in the cases in which standard correction schemes cannot be applied. Excluding the case of the relatively small 64-atom supercells, the errors of the corrected formation energies with respect to the extrapolated value in the dilute limit are smaller than 0.16 eV in all cases. Similar errors are found for the FNV scheme applied to the formation energies of regularly screened oxygen vacancies, as can be seen in the SM [17] and in agreement with the literature [7].

To highlight the role of the ionic polarization charge q'_{pol} , we focus on the $(0, \mathbf{R}_{+1})$ state of the oxygen vacancy in MgO, in which the localized charge is solely provided by the ionic polarization. In Fig. 4(a), we display the potential V_{DFT} obtained from the hybrid-functional calculation. We compare the latter with the long-range model potential associated with a charge q'_{pol} screened by ε_∞ ,

$$V_m(\mathbf{r}; q'_{\text{pol}}, \varepsilon_\infty) = \frac{1}{\varepsilon_\infty} \int d\mathbf{r}' \frac{\rho_m(\mathbf{r}'; q'_{\text{pol}})}{|\mathbf{r} - \mathbf{r}'|}, \quad (7)$$

where $\rho_m(\mathbf{r}'; q'_{\text{pol}})$ represents a Gaussian distribution of charge q'_{pol} . Figure 4(a) shows that V_{DFT} is well described by V_m in the long range, supporting the description of the ionic polarization in terms of the charge q'_{pol} . The role of q'_{pol} can be further emphasized by displaying the finite-size errors with respect to the dilute limit for $E_f(q, \mathbf{R}_{+1})$, where the charge

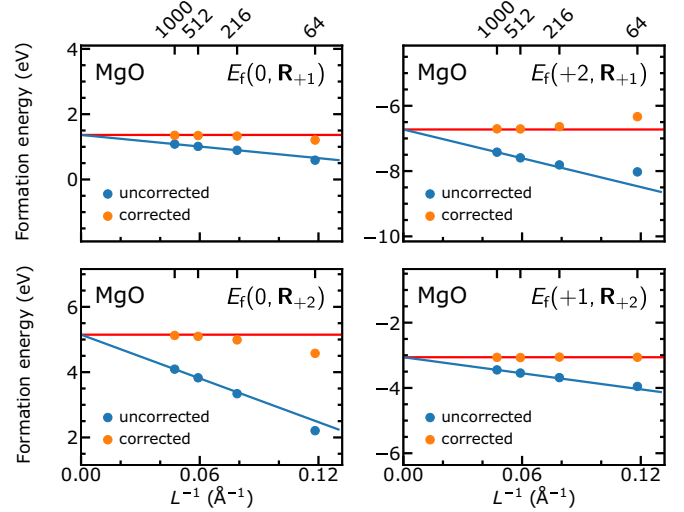


FIG. 3. Formation energies of various states $(q, \mathbf{R}_{q'})$ of the oxygen vacancy in MgO as a function of the inverse supercell size L^{-1} . The number of atoms in the supercell is given at the top. The formation energies in the dilute limit are found by linear extrapolation of the two largest supercells and are indicated by horizontal red lines. In charged systems, we take $\varepsilon_f = 0$.

states $q = 0, +1, +2$ are considered in the presence of the same frozen configuration \mathbf{R}_{+1} . In Fig. 4(b), we display these errors for every considered supercell size and interpolate them with parabola. When the supercells are sufficiently large, the minima of these parabola occur at charge $-q'_{\text{pol}}$ pertaining to \mathbf{R}_{+1} . This is consistent with our finite-size expression in Eq. (4), since the third term $E_m(q + q'_{\text{pol}}, \varepsilon_\infty)$ is quadratic in the localized charge [6,12–14] and is thus minimized for $q = -q'_{\text{pol}}$. At the minimum the electronic polarization is absent, but the correction does not vanish because of the first two terms in Eq. (4), which correspond to the establishment of the ionic polarization in the geometry \mathbf{R}_{+1} .

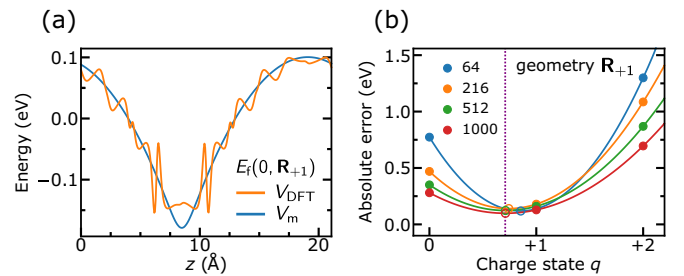


FIG. 4. (a) Comparison between the potential V_{DFT} obtained from the hybrid-functional calculation for the $(0, \mathbf{R}_{+1})$ state of the O vacancy in MgO and the model potential $V_m(\mathbf{r}; q'_{\text{pol}}, \varepsilon_\infty)$ resulting from a Gaussian distribution of charge $q'_{\text{pol}} = -(1 - \varepsilon_\infty/\varepsilon_0)$ with a width of 1 bohr. (b) Absolute finite-size error with respect to the dilute limit for $E_f(q, \mathbf{R}_{+1})$ with $q = 0, +1, +2$ (solid circles). Supercells based on various numbers of atoms are considered. The data are interpolated with parabola and the obtained minima are indicated with open circles. The vertical line indicates the charge $-q'_{\text{pol}}$ and corresponds to the theoretical minimum of the finite-size correction for \mathbf{R}_{+1} .

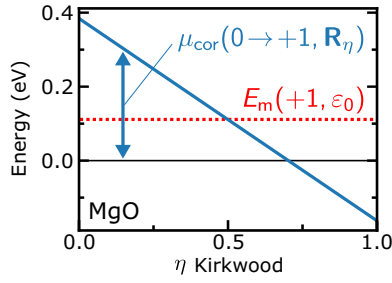


FIG. 5. Illustration of the sum rule defined in Eq. (9) for a transition between the defect charge states of $q' = 0$ and $q = +1$ in a 1000-atom supercell of MgO. For each value of the Kirkwood parameter η , the correction $\mu_{\text{cor}}(0 \rightarrow +1, \mathbf{R}_\eta)$ is evaluated through Eq. (6). The mean value of $\mu_{\text{cor}}(0 \rightarrow +1, \mathbf{R}_\eta)$ (red line) equals $E_m(+1, \varepsilon_0)$.

As a second case study, we focus on the vertical extraction energy of the hydrated electron. In the final state, the system is neutral but the structure of liquid water presents a strong dipolar polarization giving rise to significant finite-size effects (cf. Fig. 1) [4]. We take uncorrected data for the vertical transition $\mu(-1 \rightarrow 0, \mathbf{R}_{-1})$ calculated in Ref. [4] and apply our scheme based on FNV model corrections for E_m [6,30,31] (see SM [17]). We use static and high-frequency dielectric constants inferred from experimental data ($\varepsilon_0 = 78.3$ [15] and $\varepsilon_\infty = 1.78$ [32]). Compared to the extrapolated limit, our corrected transition energies show errors of 0.11 and 0.04 eV for supercells containing 64 and 128 water molecules, respectively, thereby further supporting the accuracy of our scheme [cf. Fig. 1(c)].

To corroborate the general validity of our formulation, we show that the finite-size corrections for vertical transition energies in Eq. (6) satisfy a sum rule that connects them to standard corrections of structurally relaxed defects [Eq. (2)]. To derive the sum rule, we adopt a procedure commonly utilized in the framework of the thermodynamic integration method [33–35]. To describe the transition from the charge state q' to that of q , we introduce a fictitious Hamiltonian $\mathcal{H}_\eta = \eta\mathcal{H}_q + (1 - \eta)\mathcal{H}_{q'}$, where η is the Kirkwood parameter [36], and $\mathcal{H}_{q'}$ and \mathcal{H}_q are the Hamiltonians associated with the initial and final states, respectively. This leads to

$$E(q, \mathbf{R}_q) - E(q', \mathbf{R}_{q'}) = \int_0^1 d\eta \mu(q' \rightarrow q, \mathbf{R}_\eta), \quad (8)$$

where the terms on the left-hand side correspond to equilibrium energies of relaxed defects, whereas the integrand on the right-hand side is the vertical transition energy defined in Eq. (5). This leads to the following relationship between the corresponding finite-size corrections,

$$E_m(q, \varepsilon_0) - E_m(q', \varepsilon_0) = \int_0^1 d\eta \mu_{\text{cor}}(q' \rightarrow q, \mathbf{R}_\eta). \quad (9)$$

It can be proven that this relationship is generally satisfied by our finite-size corrections for vertical charge transition energies [17]. The proof uses the quadratic dependence of the model correction $E_m(q, \varepsilon)$ on q and the linearity of the model potential $V_m(\mathbf{r}; q, \varepsilon)$ in q . An explicit derivation is given for the case of the FNV model correction [6] in the SM [17]. In

Fig. 5, we illustrate the relationship between the finite-size corrections in Eq. (9) for a transition from $q' = 0$ to $q = +1$ in MgO.

The present formulation also opens the way to the corrections for single-particle defect levels. Such corrections find immediate application when calculating quasiparticle shifts in many-body *GW* formulations [37,38] and when enforcing the generalized Koopmans' condition to defect states [3,39–43]. The Kohn-Sham level ϵ of a defect of charge q in the geometry \mathbf{R}_q can be related to its total energy $E(q, \mathbf{R}_q)$ through Janak's theorem [44],

$$\epsilon(q, \mathbf{R}_q) = - \lim_{Q \rightarrow q} \frac{\partial E(Q, \mathbf{R}_q)}{\partial Q}. \quad (10)$$

Using Eq. (4) and the quadratic dependence of $E_m(q, \varepsilon)$ on q , we find that the corresponding finite-size correction ϵ_{cor} is expressed as

$$\epsilon_{\text{cor}}(q, \mathbf{R}_q) = -2 \frac{E_m(q + q'_{\text{pol}}, \varepsilon_\infty)}{q + q'_{\text{pol}}}. \quad (11)$$

For structurally relaxed defects, i.e., when $q' = q$, the formula in Eq. (11) falls back to the expression found by Chen and Pasquarello [31] in view of the relation in Eq. (3). In the SM [17] we prove Eq. (11) and illustrate the scaling of the energy levels for the hole polaron in MgO. We remark that our scheme for single-particle energies performs as accurately as for vertical transitions, in contrast with the findings of Gake *et al.*, who used inadequate corrections for single-particle levels [16].

In conclusion, we derived finite-size corrections for vertical transition energies and single-particle energy levels involving defect states with built-in ionic polarization. The present formulation is fully general and applies to defect states in condensed systems ranging from the solid to the liquid state. Its physical motivation is transparent and the limiting cases are trivially recovered. Our method allows for the combination with existing schemes for regularly relaxed defects, making its implementation and use widely accessible [45]. Our corrections are validated through numerical case studies in MgO and water and through the analytical condition set by a sum rule. This scheme allows one to achieve accurate optical transition energies for identifying defect signatures in measured optical spectra without requiring computationally prohibitive system-size scalings.

The code for calculating finite-size corrections is provided on GitHub [45]. Additional material associated to this work can be found on Materials Cloud [46].

We acknowledge useful interactions with Francesco Ambrosio, Wei Chen, and Patrick Gono. This work has been realized in relation to the National Center of Competence in Research (NCCR) ‘‘Materials’ Revolution: Computational Design and Discovery of Novel Materials (MARVEL)’’ of the Swiss National Science Foundation. The calculations have been performed at the Swiss National Supercomputing Centre (CSCS) (grant under Projects ID s879 and mr25) and at SCITAS-EPFL.

- [1] T. R. Paudel and W. R. L. Lambrecht, *Phys. Rev. B* **77**, 205202 (2008).
- [2] D. Kan, T. Terashima, R. Kanda, A. Masuno, K. Tanaka, S. Chu, H. Kan, A. Ishizumi, Y. Kanemitsu, Y. Shimakawa *et al.*, *Nat. Mater.* **4**, 816 (2005).
- [3] P. Deák, Q. Duy Ho, F. Seemann, B. Aradi, M. Lorke, and T. Frauenheim, *Phys. Rev. B* **95**, 075208 (2017).
- [4] F. Ambrosio, G. Miceli, and A. Pasquarello, *J. Phys. Chem. Lett.* **8**, 2055 (2017).
- [5] C. Freysoldt, B. Grabowski, T. Hickel, J. Neugebauer, G. Kresse, A. Janotti, and C. G. Van de Walle, *Rev. Mod. Phys.* **86**, 253 (2014).
- [6] C. Freysoldt, J. Neugebauer, and C. G. Van de Walle, *Phys. Rev. Lett.* **102**, 016402 (2009).
- [7] H.-P. Komsa, T. T. Rantala, and A. Pasquarello, *Phys. Rev. B* **86**, 045112 (2012).
- [8] C. W. M. Castleton, A. Höglund, and S. Mirbt, *Phys. Rev. B* **73**, 035215 (2006).
- [9] N. D. M. Hine, K. Frensch, W. M. C. Foulkes, and M. W. Finnis, *Phys. Rev. B* **79**, 024112 (2009).
- [10] S. E. Taylor and F. Bruneval, *Phys. Rev. B* **84**, 075155 (2011).
- [11] C. W. M. Castleton and S. Mirbt, *Phys. Rev. B* **70**, 195202 (2004).
- [12] M. Leslie and N. J. Gillan, *J. Phys. C* **18**, 973 (1985).
- [13] G. Makov and M. C. Payne, *Phys. Rev. B* **51**, 4014 (1995).
- [14] S. Lany and A. Zunger, *Phys. Rev. B* **78**, 235104 (2008).
- [15] W. M. Haynes, *CRC Handbook of Chemistry and Physics* (CRC Press, Boca Raton, FL, 2014).
- [16] T. Gake, Y. Kumagai, C. Freysoldt, and F. Oba, *Phys. Rev. B* **101**, 020102(R) (2020).
- [17] See Supplemental Material at <http://link.aps.org/supplemental/10.1103/PhysRevB.102.041115> for computational details, extra information on finite-size errors, a comparison with previous results, the proof of the sum rule, the comparison with other correction schemes for vertical transitions, and corrections of single-particle defect levels.
- [18] J. P. Perdew, M. Ernzerhof, and K. Burke, *J. Chem. Phys.* **105**, 9982 (1996).
- [19] J. VandeVondele, M. Krack, F. Mohamed, M. Parrinello, T. Chassaing, and J. Hutter, *Comput. Phys. Commun.* **167**, 103 (2005).
- [20] S. Goedecker, M. Teter, and J. Hutter, *Phys. Rev. B* **54**, 1703 (1996).
- [21] C. Hartwigsen, S. Goedecker, and J. Hutter, *Phys. Rev. B* **58**, 3641 (1998).
- [22] J. VandeVondele and J. Hutter, *J. Chem. Phys.* **127**, 114105 (2007).
- [23] M. Guidon, J. Hutter, and J. VandeVondele, *J. Chem. Theory Comput.* **6**, 2348 (2010).
- [24] R. Whited, C. J. Flaten, and W. Walker, *Solid State Commun.* **13**, 1903 (1973).
- [25] J. B. Varley, A. Janotti, C. Franchini, and C. G. Van de Walle, *Phys. Rev. B* **85**, 081109(R) (2012).
- [26] P. Rinke, A. Schleife, E. Kioupakis, A. Janotti, C. Rödl, F. Bechstedt, M. Scheffler, and C. G. Van de Walle, *Phys. Rev. Lett.* **108**, 126404 (2012).
- [27] P. Umari and A. Pasquarello, *Phys. Rev. Lett.* **89**, 157602 (2002).
- [28] R. C. Whited and W. C. Walker, *Phys. Rev. Lett.* **22**, 1428 (1969).
- [29] J. A. Van Vechten, *Phys. Rev.* **182**, 891 (1969).
- [30] C. Freysoldt, J. Neugebauer, and C. G. Van de Walle, *Phys. Status Solidi B* **248**, 1067 (2011).
- [31] W. Chen and A. Pasquarello, *Phys. Rev. B* **88**, 115104 (2013).
- [32] I. Thormählen, J. Straub, and U. Grigull, *Phys. Chem. Ref. Data* **14**, 933 (1985).
- [33] D. Frenkel and B. Smit, *Understanding Molecular Simulation: From Algorithms to Applications* (Elsevier, San Diego, 1996).
- [34] J. Cheng, M. Sulpizi, and M. Sprik, *J. Chem. Phys.* **131**, 154504 (2009).
- [35] F. Ambrosio, G. Miceli, and A. Pasquarello, *J. Chem. Phys.* **143**, 244508 (2015).
- [36] J. G. Kirkwood, *J. Chem. Phys.* **3**, 300 (1935).
- [37] W. Chen and A. Pasquarello, *J. Phys.: Condens. Matter* **27**, 133202 (2015).
- [38] M. Jain, J. R. Chelikowsky, and S. G. Louie, *Phys. Rev. Lett.* **107**, 216803 (2011).
- [39] G. Miceli, W. Chen, I. Reshetnyak, and A. Pasquarello, *Phys. Rev. B* **97**, 121112(R) (2018).
- [40] S. Kokott, S. V. Levchenko, P. Rinke, and M. Scheffler, *New J. Phys.* **20**, 033023 (2018).
- [41] B. Sadigh, P. Erhart, and D. Åberg, *Phys. Rev. B* **92**, 075202 (2015).
- [42] T. J. Smart, F. Wu, M. Govoni, and Y. Ping, *Phys. Rev. Mater.* **2**, 124002 (2018).
- [43] T. Bischoff, I. Reshetnyak, and A. Pasquarello, *Phys. Rev. B* **99**, 201114(R) (2019).
- [44] J. F. Janak, *Phys. Rev. B* **18**, 7165 (1978).
- [45] S. Falletta, J. Wiktor, and A. Pasquarello (2020), <https://github.com/falletta/finite-size-corrections-defect-levels>.
- [46] S. Falletta, J. Wiktor, and A. Pasquarello (2020), [10.24435/materialscloud:9p-g7](https://doi.org/10.24435/materialscloud:9p-g7).